

# Surface processing with gas-cluster ions to improve giant magnetoresistance films

D. B. Fenner,<sup>a)</sup> J. Hautala, L. P. Allen, and T. G. Tetreault  
*Epion Corporation, Billerica, Massachusetts 01821*

A. Al-Jibouri  
*Nordiko Limited, Hampshire P09 2NL, England*

J. I. Budnick  
*Department of Physics, University of Connecticut, Storrs, Connecticut 06269*

K. S. Jones  
*Department of Materials Science, University of Florida, Gainesville, Florida 32611*

(Received 11 September 2000; accepted 20 November 2000)

The reduction of roughness, without introducing damage, of thin-film surfaces in giant magnetoresistance (GMR) applications will be essential in the development of advanced devices. Tools and methods to accomplish this are limited at present. Gas-cluster ion beam (GCIB) technology shows promise as a dry, low-temperature process that can provide substantial improvement, and can be integrated into GMR-film deposition-and-etch tools. In this work, we describe recent GCIB technique developments and processes for tantalum, alumina, permalloy, and other relevant materials. With argon GCIB it is possible to reduce the roughness of many films to well below a nanometer (root-mean-square), with the roughness falling exponentially with cluster dose. Prototype magnetic films for evaluation were fabricated on GCIB-smoothed alumina gap layers. Transmission electron microscopy revealed changes in roughness and grain morphology that may be correlated with magnetic properties. © 2001 American Vacuum Society.  
[DOI: 10.1116/1.1349193]

## I. INTRODUCTION

The role of bulk and surface defects in thin-film technology has been of great interest in both science and applications since the beginning of modern methods of film deposition and etching. Present technologies progressively require films that are thinner and of higher quality, becoming a significant challenge to the fabrication technology industry. The requirements of abrupt interfaces and fine-grained metal morphology for films in giant magnetoresistance (GMR) sensor devices,<sup>1-5</sup> virtually eliminates any high-temperature or high kinetic-energy film-deposition processes. Those processes typically bring important advantages that include diffusion-smoothed surfaces and defect reduction by annealing. Fabrication of GMR devices on certain ceramic substrates and on thick magnetic-shield layers likewise adds complications, including rough surfaces. Technologies for the market often demand specific materials that, when deposited, are rough at the nanometer scale. There are few satisfactory tools available for removing this roughness (i.e., smoothing).

Wet methods such as chemical-mechanical polishing (CMP) are difficult to implement at the low level of surface roughness and polishing-induced defects required by future generations of GMR-like devices. Conventional ion-plasma and ion-beam sputtering and etching methods have significant drawbacks for GMR device manufacturing.<sup>2,6-9</sup> Induced roughness and ion damage are limitations for all but the

smallest ion doses. A method is desired and gas-cluster ion beam (GCIB) processing may provide that. This technique, which is described in detail elsewhere,<sup>10-12</sup> consists of apparatus to inject high-pressure argon gas through an expansion nozzle into vacuum, which causes condensation droplets to form. These droplets, or clusters, are quickly frozen and form into a jet of solid nanoparticles. The jet is ionized by passage through a low-voltage electron beam resulting in predominantly singly and positively charged clusters. Extraction and acceleration through a high voltage result in the GCIB, which is then suitable for surface processing when incident normal to the surface. Since the cluster condensation thermodynamics occurring in the nozzle results in a wide distribution of cluster sizes, peaked at very roughly 2000 atoms each, and a typical acceleration potential is 20 kV, the argon atoms within each cluster have an average energy of only ~10 eV upon impact.

The reduction of surface roughness by exposure to a GCIB, occurs by virtue of physical mechanisms that are different from those of conventional ion-beam bombardment.<sup>11,12</sup> The large size of clusters (relative to molecular dimensions), the very low bonding energy, and the low kinetic energy per atom, result in a highly inelastic collision, dominated by cooperative phenomena within the cluster as it undergoes breakup upon striking the solid (strongly bound) target surface. Atoms from argon clusters do not significantly penetrate the surface. Thus, any induced damage after multiple cluster collisions is estimated to be confined to approximately the outermost 1 nm. However, as the clusters

<sup>a)</sup>Electronic mail: dfenner@epion.com

exit the impact site there is a tendency for the surface material to leave at fairly shallow angles from the surface.<sup>11,12</sup> Further, those clusters that strike an inclined surface (perhaps at sites of local tilt due to roughness) cause more material to be displaced down slope rather than up. The net effect is that rough surfaces tend to become smooth with GCIB exposure, and surface asperities and contamination are rapidly removed. In particular, features with spatial frequency that is high, but less than that associated with the size of a cluster, are preferentially removed. Argon-GCIB exposure has been observed to result in smoothing for a wide variety of inorganic materials, including those used in microelectronic and photonic technologies.<sup>11-13</sup>

To be useful, surface etching and smoothing must not substantially increase the coercive field ( $H_c$ ) of the ferromagnetic free layer, cause layer intermixing within the sensor layers, nor reduce the exchange field between the pinned and antiferromagnetic layers. It is intended that smoothing reduce the magnetostatic coupling of the free and pinned layers and improve the specular reflection of electrons within the spacer layer.<sup>14</sup> In this article we describe recent efforts to understand the effects on roughness, microstructure and magnetic properties of very thin metal films deposited onto substrates or films that are smoothed by GCIB. To this end, we have assembled a coupled vacuum system with both film deposition and GCIB smoothing capabilities. Various samples were fabricated and characterized with the integrated tool. In particular, we have focused at this stage on a study of the effect of smoothing alumina gap layers within a simple GMR-type of film stack.

## II. RESULTS AND DISCUSSION

Silicon wafer surfaces have been exposed to GCIB for assessment of beam effects, as described previously.<sup>12,13,15</sup> Roughness reduction is not a requirement for silicon to be used as a substrate since conventional manufacturing is able to produce very low roughness wafers. However, GCIB exposure of silicon does not introduce measurable damage or contamination as evidenced by the lack of change in the surface topography as seen with an atomic force microscope (AFM), and the absence of foreign elements found with total reflection x-ray fluorescence. Some oxidation of the silicon is observed if the argon beam acts in a process chamber with base pressure of  $1 \times 10^{-7}$  Torr or above, and this is under further study.

Substrates of AlTiC ( $\text{Al}_2\text{O}_3$ -TiC ceramic) with surfaces previously polished by CMP were exposed to argon-GCIB and then compared with the unexposed surfaces. Characterization with AFM and scanning Auger microscope (SAM) revealed the topography and composition, respectively. Prior to GCIB exposure, the ceramic surface is composed of TiC grains, a few microns in size, within an alumina matrix. These TiC grains are often raised above the matrix material a few nanometers or more, even after CMP. As can be seen in Fig. 1, after GCIB exposure the protrusion of the grains is considerably reduced in the AFM images, without any observable change in the SAM composition images. The aver-

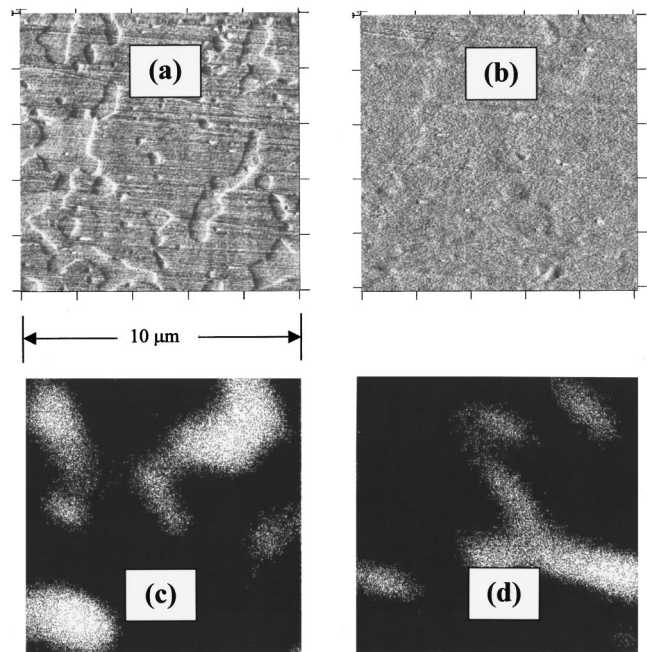


FIG. 1. Micrograph images of the surface of an AlTiC wafer prior to (a),(c) and after (b),(d) exposure to argon-GCIB with dose of  $4 \times 10^{15}$  ions/cm<sup>2</sup>. Topography is shown by the AFM images in (a) and (b), where the areas scanned are  $10 \times 10 \mu\text{m}^2$ , and the gray scale is 5 nm. Composition is shown by the SAM images in (c) and (d), where the white regions are rich in Ti and the areas scanned are  $20 \times 20 \mu\text{m}^2$ .

age roughness ( $R_a$ ) of the surface was reduced by a factor of 2, attaining  $R_a < 3 \text{ \AA}$ . The escape depth of the Ti Auger electrons is estimated to be  $\sim 1$  nm, however, lateral resolution is limited to  $\sim 1 \mu\text{m}$ .

Films of permalloy and sendust (Ni/Fe and Fe/Si alloys, respectively) have been evaluated for response to the GCIB process.<sup>12,13</sup> Permalloy materials of both thick, electroplated films (intended for use as GMR-device shield layers), and thin films (intended for use as free or pinned sensor layers) were evaluated. The thick films had received a CMP final treatment (typical of vendor process) and with AFM were found to have distinct scratch and dig marks in addition to a more random and uniform roughness. Argon-GCIB processing eliminates most of the scratch marks visible in AFM images and substantially reduces the random roughness. Figures 2(a) and 2(b) show perspective-view AFM images of such surfaces before and after GCIB exposure. Ongoing work is being done to characterize the extent to which residual damage layers remaining after the final CMP can be removed by the GCIB process. The GCIB process is intrinsically a stable etch when acting on a flat surface, i.e., to the extent that a surface is smooth, it does not become progressively rough again as the beam acts on the surface. Thus, it is expected that thin damage layers can be removed (etched away) without reintroducing damage due to the action of the cluster beam. On most surfaces, etch stability of GCIB processing has been observed. However, films with void defects, high stress (as deposited), or high chemical reactivity are not so well behaved. For example, thin films of permalloy deposited on very smooth, thermally oxidized silicon wafers

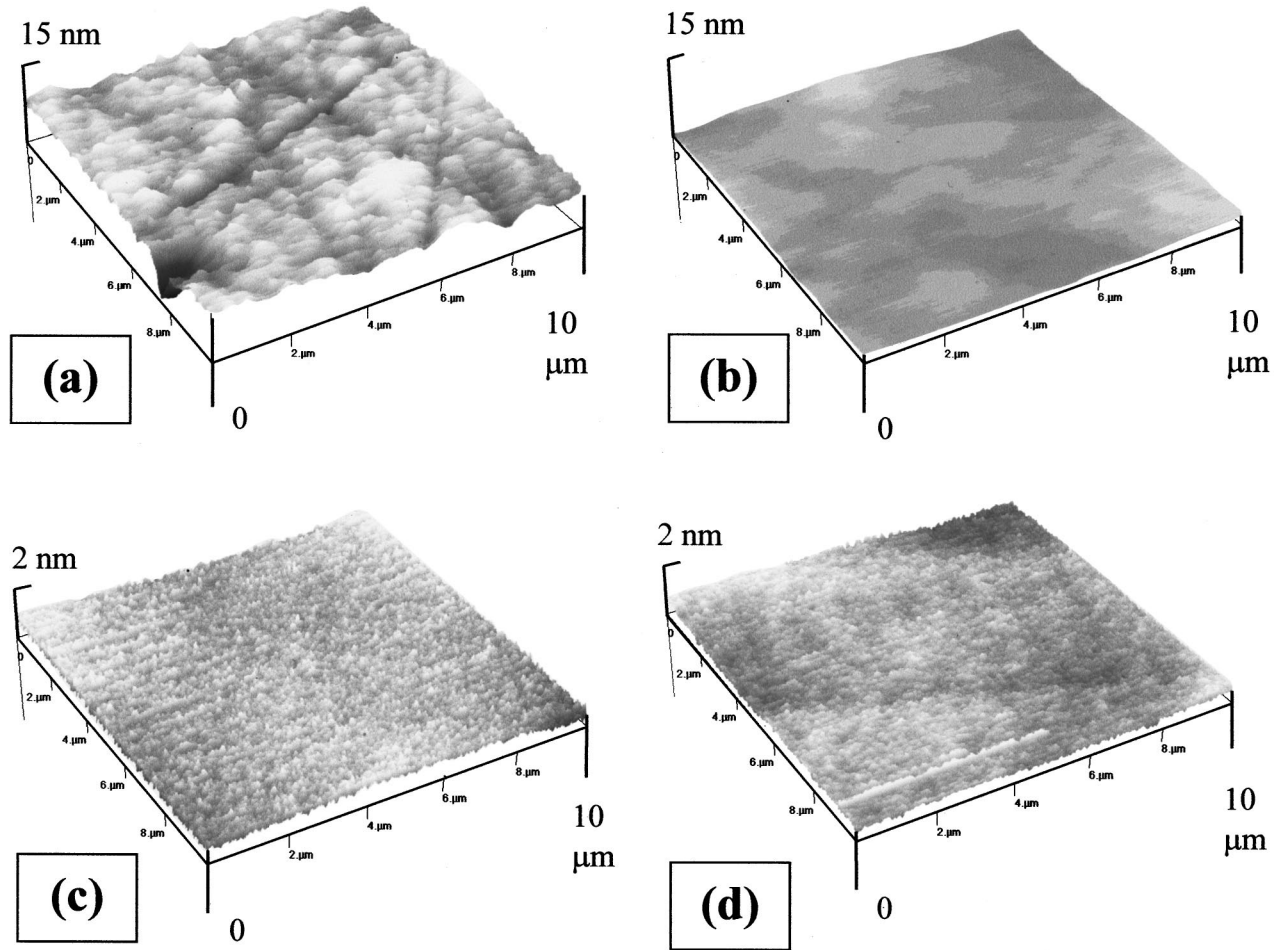


FIG. 2. AFM micrograph images of the surface of permalloy films prior to (a),(c) and after (b),(d) exposure to argon-GCIB with dose of  $2 \times 10^{15}$  ions/cm<sup>2</sup>. The AFM images in (a) and (b) are of a thick electrodeposited permalloy (see Ref. 12), while those in (c) and (d) are thin films on very smooth silicon. The areas scanned are  $10 \times 10 \mu\text{m}^2$ , and the gray scale is 2 nm.

are themselves quite smooth and defect free. Exposure of these films to argon GCIB in a typical process as used for smoothing rough films, does not change the roughness of these very smooth films. Figures 2(c) and 2(d) show perspective-view AFM images of such a smooth permalloy, as deposited, and after GCIB dose of  $2 \times 10^{15}$  ions/cm<sup>2</sup>. Both before and after GCIB, the films have  $R_a \sim 1 \text{ \AA}$ .

The gap layer in a GMR device typically consists of a deposited alumina film, and smoothing of these films by use of GCIB was reported previously.<sup>13</sup> A smooth surface texture (as observed by AFM) is important but not a sufficient indicator for use of such a film underneath a GMR sensor. In order to understand what effect the smoothing of a gap layer may have on subsequently deposited, overlying films, we have deposited seed layers of Ta on the gap films and evaluated the Ta surface. So as to reduce the possibility of damage or contamination, the work was done with an integrated tool set consisting of a GCIB smoothing system and a (physical vapor) metal-film deposition station and vacuum transfer apparatus. This integrated tool was assembled at the Nordiko facility. Further, a set of four AlTiC wafers each with shield and gap layers was studied. Two wafers had a higher-polish

grade of the thick permalloy shield layers and two had a lower-grade polish. All four had alumina gap layers deposited under nominally identical conditions. One wafer from each pair was processed with GCIB and then immediately capped with Ta films 500 Å in thickness, while the other pair were capped in the same process lot but without GCIB processing. All the surfaces of the gap layers were checked by AFM prior to processing in the integrated tool and then the surfaces of the Ta caps were evaluated afterwards. The gap films began with roughness in the range of  $R_a \sim 30\text{--}40 \text{ \AA}$  on one pair, and  $R_a \sim 9\text{--}10 \text{ \AA}$  on the other pair. Without GCIB, deposition of a Ta cap layer essentially left unchanged the surface roughness on both types, i.e.,  $R_a \sim 30 \text{ \AA}$  and  $R_a \sim 9 \text{ \AA}$  of the Ta surfaces. The other pair received an exposure of  $1 \times 10^{15}$  ions/cm<sup>2</sup> of ionized clusters (composed of argon) accelerated by 14 kV,<sup>11-13</sup> and the final Ta-cap layer surfaces were found to have significantly less roughness,  $R_a \sim 20 \text{ \AA}$  and  $R_a \sim 5 \text{ \AA}$ , respectively. Figure 3 shows AFM plan-view images and typical cross sections of the wafer pair that began rougher, one of which was just capped and the other of which received the GCIB exposure and then the cap. Clearly, the Ta film topology has been improved, and in this

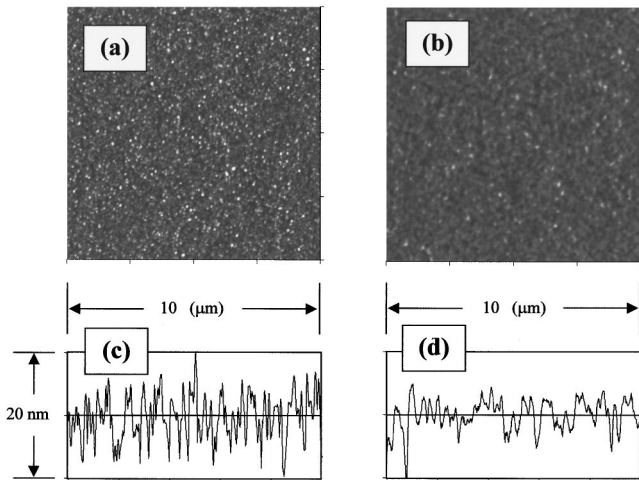


FIG. 3. AFM micrograph images of the surfaces of Ta films on initially rough alumina gap layers, without (a),(c) and with (b),(d) exposure of the alumina to argon-GCIB at a dose of  $1 \times 10^{15}$  ions/cm<sup>2</sup>. In (a) and (b) are plan views and in (c) and (d) are typical cross sections (or height profiles). The areas scanned are  $10 \times 10 \mu\text{m}^2$ , and the gray scale is 20 nm. In (a) the  $R_a \sim 30 \text{ \AA}$ , and in (b)  $R_a \sim 20 \text{ \AA}$ .

respect would seem to be more suitable as a seed layer below a GMR film stack.

One requirement for GCIB smoothing to be a useful process of any surface below the sensor stack, is that it not cause a substantial increase in  $H_c$  of a permalloy free layer. Prototype free layers of permalloy were fabricated on four silicon wafers, and for each of these the permalloy layer was preceded and followed by thin Ta layers, forming trilayer stacks of Ta/NiFe/Ta. All film depositions and argon-GCIB exposures were done with the integrated tool described earlier. First, a reference sample (No. 1) consisting of a trilayer was fabricated on a smooth silicon wafer. Second, a trilayer sample (No. 2) was fabricated on an alumina gap layer (500 Å) deposited on a thick Cu layer that was, because of its thickness (3000 Å), somewhat rough. Third, a trilayer sample (No. 3) was fabricated on the identical gap layer (on rough Cu, as before), but prior to deposition of this trilayer the gap alumina was smoothed by GCIB processing. Fourth, a sample (No. 4) was fabricated by repeating the process of sample No. 3 just described, but this time the bottom Ta layer (which is immediately on top of the GCIB-processed alumina) was made tenfold thicker.

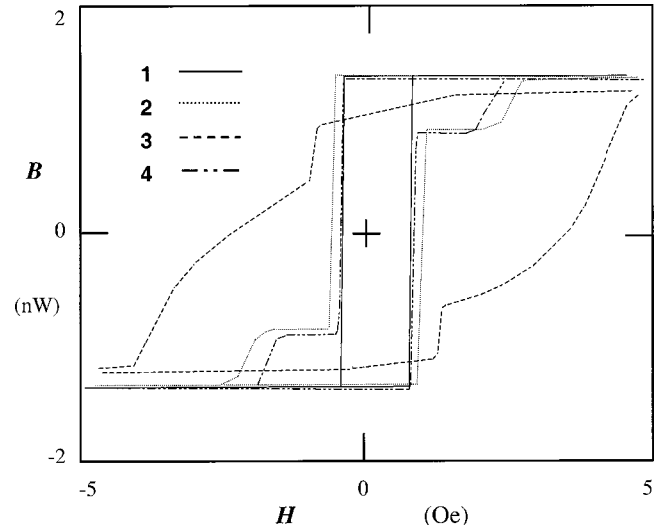


FIG. 4. Magnetic hysteresis loops for a series of permalloy films on various substrates, as listed in Table I. The four loops are labeled according to that table.

Finally, magnetic hysteresis  $B(H)$  loops were measured for these permalloy films and the coercivity field ( $H_c$ ) of each was determined. These measurements were made using the entire 150 mm diameter wafers, and with a driving alternating current field of 10 Hz.<sup>16</sup> The sample descriptions and measured  $H_c$  values are listed in Table I. In Fig. 4 are shown the magnetization loops for these four samples. Some discussion is in order. The sample No. 1 was fabricated as a reference as to the quality possible for the permalloy films in this fabrication set. That substrate is very smooth and no other films were inserted below the Ta/NiFe/Ti trilayer, thus ensuring optimum conditions. Indeed, for this sample the observed  $B(H)$  loop was very square and the measured  $H_c$  was quite small. The other three samples were intentionally roughened to simulate the more typical AlTiC wafer and/or CMP-processed shield layer. Moderate roughening ( $R_a \sim 30 \text{ \AA}$ ) was accomplished by deposition of the thick Cu films. Sample No. 2 facilitated observation of the effect of increased roughness on the  $B(H)$  loop, and a modest increase in  $H_c$  was measured. As seen in Fig. 4, the loop for sample No. 2 (like those of Nos. 3 and 4) is composed of two components, one generally square in shape and the other adding shoulders to the square. Each of the metal films was

TABLE I. Sample set fabricated to evaluate the effect of GCIB smoothing of alumina gap layers upon the coercivity field of overlying permalloy thin films. Sample No. 1 is for reference only and contains no gap layer. The  $H_c$  field is the half width of the main loop measured for each film. The ion dose (ions/cm<sup>2</sup>) is current fluence, not atom-number fluence.

No.	Base structure	GCIB process	Trilayers and thicknesses (Å)	Coercivity field $H_c$ (Oe)
1	Si wafer, smooth	None	Ta 50/NiFe 100/Ta 50	0.58
2	Si/Cu/Al <sub>2</sub> O <sub>3</sub> , rough	None	Ta 50/NiFe 100/Ta 50	0.79
3	Si/Cu/Al <sub>2</sub> O <sub>3</sub> , rough	$4 \times 10^{15}$ ions/cm <sup>2</sup>	Ta 50/NiFe 100/Ta 50	$\sim 3.0$
4	Si/Cu/Al <sub>2</sub> O <sub>3</sub> , rough	$4 \times 10^{15}$ ions/cm <sup>2</sup>	Ta 500/NiFe 100/Ta 50	0.63

deposited to cover uniformly an entire 150 mm diameter wafer, however, the alumina deposition was limited to 125 mm diameter. Thus, the entire perimeter of sample Nos. 2–4 have a wide band without alumina, where the copper film directly contacts the permalloy and thus shunts current induced by the hysteresis-loop measurement apparatus. After all of the  $B(H)$  loops were measured, one of the samples was coarsely cleaved to remove the edges and then re-evaluated, whereupon the shoulders were found to be absent from the loop.

The  $B(H)$  loop observed for sample No. 3 is quite wide, as is evident in Fig. 4. With this sample the alumina surface was exposed to argon GCIB, which resulted in severely degraded magnetic properties of the overlying permalloy film (which the beam never interacted with directly). Several mechanisms for damage might be hypothesized, including beam-induced defects or stoichiometry shifts in the alumina, or alterations in the microstructure or surface chemistry that causes changes in the nucleation and growth properties of the Ta film during its deposition. Any such mechanism might then cause at least some changes in the permalloy microstructure, away from the fine-grained, face-centered-cubic (111) orientation of the polycrystalline film.<sup>1,4,14</sup> The  $B(H)$  loop observed for sample No. 4 gives some indication of the cause of the problem observed in No. 3, since with the thicker bottom Ta layer in No. 4 the narrow  $B(H)$  loop is restored. In fact, the measured  $H_c$  for No. 4 is smaller than that for No. 2, suggesting that the roughness reduction has caused an improvement in the permalloy coercivity, or at a minimum has not made it substantially worse. Sample No. 4 has a rather thick (500 Å) bottom Ta layer and it is anticipated that with additional work it will be found that Ta seed films thinner than this will suffice to provide low coercivity in the permalloy. It is expected that grain growth starting on smoother alumina will have a lower nucleation density, which will result in larger grains upon coalescence. In No. 4, the bottom Ta film was grown on smoothed alumina but was perhaps now thick enough to allow the Ta grains to coalesce, resulting in a microstructure more akin to that on the rougher substrate (No. 2). Closely related may be the possibility that very thin Ta on smoothed alumina (No. 3) will have a high density of pinholes in it due to the Ta grains not having fully coalesced. In either case, the solution may well be to add an additional, but very thin buffer layer between the smoothed alumina and a conventional (thin) Ta layer, to restore the desired grain morphology.

The effect of GCIB smoothing of gap layers on the grain structure of overlying antiferromagnetic layers was also studied. For this, two additional thin-film samples on silicon, similar to those listed in Table I, were fabricated with the integrated tool. These had under layers of thick (3000 Å) and thus rough copper, alumina gap layers (2000 Å thick), Ta seed layers (30 Å thick), PtMn (300 Å thick), and additional thin metal layers that served as cap layers. One sample was fabricated in the usual manner and for another the alumina layer was exposed to an argon–GCIB dose of  $1 \times 10^{16}$  ions/cm<sup>2</sup>. After deposition, and without annealing the

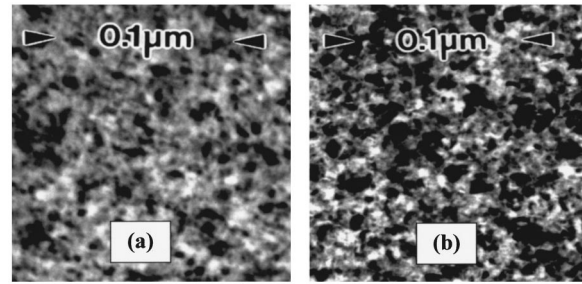


Fig. 5. Plan-view TEM images of PtMn films. In (a) the alumina layer underneath was used as deposited, while in (b) that film layer received a GCIB dose for smoothing.

PtMn layer, the top surfaces of the film stacks were measured by AFM and the average roughness of the GCIB treated sample was observed to be  $R_a \sim 5$  Å, about half the roughness of the untreated sample. Then portions of these two samples were thinned and imaged in plan view with a JEOL 200CX transmission electron microscope (TEM) using bright field imaging conditions. The thinning was done in such a fashion that the PtMn layers could be imaged, and representative micrographs are shown in Fig. 5. It can be seen that the grain microstructure is somewhat different in these two samples. Without the GCIB smoothing the grain size ranged from about 50 to 125 Å, while the GCIB smoothed sample was observed to have grain diameters ranging to larger than  $\sim 300$  Å. Also, there was no indication of any substantial change in the predominant grain orientations with GCIB exposure. Glancing-angle x-ray diffraction (XRD) was measured on these two samples, also. The PtMn(111) peaks in  $\theta$ – $2\theta$  scans were at  $39.96^\circ$  and  $40.05^\circ$  for the as-deposited and smoothed samples, respectively. In addition, this peak was somewhat narrower and stronger in the smoothed sample, indicating larger grains. Rocking ( $\omega$ ) curves indicated very little preferred alignment in either sample. Thus, both the TEM and XRD data suggest that the nucleation of grains on the smoother alumina surface resulted in larger grains in the PtMn film than for the somewhat rougher alumina.<sup>14</sup>

### III. CONCLUSIONS

The work reported here has shown promise for improving the surfaces and interfaces of thin films in GMR sensor devices by GCIB processing of substrates and structural film layers below the sensor stack. In particular, films of alumina, suitable for use as the gap layer, were smoothed by GCIB and immediately coated with seed layers of Ta using an integrated vacuum tool set. The effect of that smoothing on the Ta layer and subsequently deposited prototype sensor layers was investigated. The surface roughness of the Ta layer fabricated in the integrated tool was considerably reduced if the alumina surface received GCIB processing. Trilayers of Ta/NiFe/Ta deposited on the smoothed alumina gap layer were found to have increased coercivity if the bottom Ta layer was kept very thin and its deposition process unaltered. However, if the Ta film was made significantly thicker, then low coer-

civity was restored to the permalloy layer. Films of PtMn were deposited on the Ta seed layers overlying smoothed alumina gap layers. The grain structure of these, as deposited, was then investigated by TEM and XRD, which revealed modest increases in the grain size.

We propose that the changes in permalloy coercivity and PtMn grain morphology that were observed when these films were deposited on the smoothed alumina (with Ta seed layers), are consistent with grain nucleation and growth models. Grain nucleation density will generally be lower on smoother surfaces than on rougher surfaces. Complete coalescence of the grains and return to the desired microstructure will then require somewhat thicker films, or other modifications (e.g., additional thin buffer layers), on the smooth surface. It remains unknown to what extent fine-grained films can be smoothed (by any method) to an arbitrary level without changing their grain structure or grain nucleation properties. It is expected that completed GMR devices fabricated on smoothed sublayers (e.g., gap or shield layers) will provide superior overall performance if the appropriate changes in structure or process can be determined.

#### ACKNOWLEDGMENTS

The work at Epion was supported by DoC-NIST under ATP (70NANB8H4011). Additional support for this project came from the Marubun Corp. Assistance by W. R. Brooks,

R. J. Chandonnet, M. Davis, E. Degenkolb, V. DiFilippo, K. Gable, J. A. Greer, N. Ishikawa, S. W. Kew, A. R. Kirkpatrick, M. Mack, R. MacCrimmon, D. Rosser, W. J. Skinner, R. P. Torti, and D. Wrigley is gratefully acknowledged.

<sup>1</sup>G. Choe and M. Steinback, *J. Appl. Phys.* **85**, 5777 (1999).

<sup>2</sup>M. Li, G.-C. Wang, and H.-G. Min, *J. Appl. Phys.* **83**, 5313 (1998).

<sup>3</sup>J. C. S. Kools, W. Kula, D. Mauri, and T. Lin, *J. Appl. Phys.* **85**, 4466 (1999).

<sup>4</sup>A. S. Edelstein, K. M. Bussmann, D. C. Turner, and H. D. Chopra, *J. Appl. Phys.* **83**, 4848 (1998).

<sup>5</sup>W. F. Egelhoff *et al.*, *Mater. Res. Soc. Symp. Proc.* **517**, 9 (1998).

<sup>6</sup>J. C. S. Kools, *J. Appl. Phys.* **77**, 2993 (1995).

<sup>7</sup>M. V. R. Murty, B. Cowles, and B. H. Cooper, *Surf. Sci.* **415**, 328 (1998).

<sup>8</sup>S. D. Kim, J. J. Lee, S. H. Lim, and H. J. Kim, *J. Appl. Phys.* **85**, 5992 (1999).

<sup>9</sup>T. Mewes, R. Lopusnik, J. Fassbender, B. Hillebrands, M. Jung, D. Engel, A. Ehresmann, and H. Schmoranzler, *Appl. Phys. Lett.* **76**, 1057 (2000).

<sup>10</sup>E. W. Becker, K. Bier, and W. Henkes, *Z. Phys.* **146**, 133 (1956).

<sup>11</sup>I. Yamada and J. Matsuo, *Mater. Res. Soc. Symp. Proc.* **396**, 149 (1996).

<sup>12</sup>D. B. Fenner, R. P. Torti, L. P. Allen, N. Toyoda, A. R. Kirkpatrick, J. A. Greer, V. DiFilippo, and J. Hautala, *Mater. Res. Soc. Symp. Proc.* **585**, 27 (2000).

<sup>13</sup>D. B. Fenner, J. Hautala, L. P. Allen, J. A. Greer, W. J. Skinner, and J. I. Budnick, *Mater. Res. Soc. Symp. Proc.* (in press).

<sup>14</sup>C. Liu, C. Yu, H. Jiang, L. Shen, C. Alexander, and G. J. Mankey, *J. Appl. Phys.* **87**, 6644 (2000).

<sup>15</sup>L. P. Allen, D. B. Fenner, W. J. Skinner, R. Chandonnet, S. E. Deziel, R. P. Torti, and N. Toyoda, *IEEE Int. SOI Conf.*, Oct. 1999, Sonoma, CA, p. 116.

<sup>16</sup>SHB Instruments, model 109, hysteresis loop tracer.